JOURNAL OF CATALYSIS 136, 446–462 (1992)

Study of the Mechanism of the Cracking of Small Alkane Molecules on HY Zeolites

PRASAD V. SHERTUKDE,* GEORGE MARCELIN,* GUSTAVE A. SILL,† AND W. KEITH HALL†,[1]

*Chemical and Petroleum Engineering Department and †Department of Chemistry, University of Pittsburgh, Pittsburgh, Pennsylvania 15260

Received October 9, 1991; revised January 13, 1992

Cracking of i-butane and *n*-pentane was studied on HY zeolites. These reactions were initiated by the protonation of C–H and C–C bonds by the Brønsted acid sites. The pentacoordinated carbonium ions thus formed decomposed into carbenium ions and the products of the initiation reactions, viz., H_2, CH_4, and C_2H_6. These carbenium ions propagated chain reactions, mainly by isomerization followed by hydride transfer. Disproportionation occurred concomitantly. For these small alkanes the contribution of β-scission to product formation was negligible. "Chain length" (the number of chain cycles per initiation) was defined as the ratio of reactant molecules consumed by hydride transfer to those reacted by protonation, i.e., the ratio of rates of bimolecular propagation to unimolecular initiation. Thus, chain length reflected the average lifetime of the carbenium ions. The extent of protonation was found to increase with the strength of acid sites while the chain length remained relatively constant for preparations of a similar nature. The product distribution obtained was therefore critically dependent on the steady-state population of carbonium ions. Finally the chain reactions were terminated by decomposition of carbenium ions into corresponding alkenes. Mass balances derived from these initiation, propagation, and termination steps were in agreement for both the substrates. The product distributions obtained for i-butane and *n*-pentane cracking were satisfactorily explained on this basis.

INTRODUCTION

Recently, a considerable effort has been made to define the mechanism of cracking of small alkane molecules on HY zeolites (*1–8*). With i-butane at low conversions the problem can be understood in terms of initiation by protonation, followed by a carbenium ion chain process propagated by hydride transfer, and chain termination by the formation of alkenes. Several studies show the effect of lattice alumina, extralattice alumina, and residual base exchange cations on the activity and selectivity in these reactions over hydrogen zeolites (*1–12*). In the present work we have used the cracking of i-butane and *n*-pentane over HY zeolites to develop a better understanding of the reaction chemistry. Because of the restricted number of possible reactions, the i-butane (*2–5, 7*) and *n*-butane (*4c*) data are easy to interpret. The mechanistic picture developed using cracking of the butanes has been successfully extended to the cracking of *n*-pentane, which is somewhat more complex. The overall reaction chemistry has been systematically categorized among different initiation, propagation, and termination steps.

The protons of the Brønsted sites in HY zeolites attack C–C and C–H bonds of the reacting hydrocarbons generating pentacoordinated carbonium ions (*1–6, 13, 14*). These carbonium ions decompose into corresponding carbenium ions and the products of the initiation reaction such as H_2, CH_4 (*1–6*), and with *n*-pentane, C_2H_6. The tertiary hydrogen present in i-butane can be easily protonated. Thus, a large proportion of the reaction can be initiated with the formation of hydrogen, but CH_4 is also formed. These reactions result in the formation of

[1] To whom correspondence should be addressed.

0021-9517/92 $5.00

the *t*-butyl and 2-propyl carbenium ions, respectively. Only a restricted number of reactions are possible during i-butane cracking. This makes kinetic analysis of the product distribution tractable (*4, 7*).

Primary and secondary, but no tertiary hydrogens, are present in *n*-pentane. Studies using neopentane have indicated that the primary hydrogens are not attacked by protons of the Brønsted sites (*2, 3*). The C–H bonds of secondary hydrogens, in principle, could be protonated generating hydrogen and secpentyl carbenium ions. However, except for the first few minutes of reaction, this was not observed in the present work. So initiation of the cracking reaction of *n*-pentane must have occurred mainly by the attack on C–C bonds, generating CH_4 and C_2H_6 and their corresponding C_4 and C_3 carbenium ions.

Interestingly, even though the secondary C–H bonds were not attacked by acid sites, they must undergo H^- transfer. The reaction propagates as the carbenium ions generated on the acid sites react by H^- transfer from the reactant *n*-pentane, generating an alkane and a new C_5 carbenium ion. In this way a chain reaction is established and the "chain length" may be defined as a ratio of the rates of propagation to initiation. However, since the rate of initiation must be equal to the rate of termination in the steady state, this is also the rate of propagation divided by the rate of termination (which at low conversion may be equated to the rate of alkene formation). Thus, chain length reflects the lifetime of the carbenium ion, i.e., its steady-state concentration on the surface. This depends on the combined effect of the stability of the carbenium ion and the ease of its formation by a protonation of alkane. The present work delineates the importance of these factors in determining the product distribution.

EXPERIMENTAL

Materials

The HY zeolites used and their preparation history are described elsewhere (*9*). These zeolites can be categorized into three different groups according to their origin. The group called LZY is composed of commercial Y zeolites obtained from Linde. LZY-82 is an ultrastable HY zeolite presumably prepared by deep-bed steaming and is treated separately in this work. The LZY-210-(6, 9, and 12) series were all structurally pure NH_4Y zeolites while LZY-62 contained a small amount of nonframework octahedral alumina.

Two other series of Y zeolites called DY and SY zeolites were prepared by using ammonium hexafluorosilicate dealumination of LZY-62 and by steaming of LZY-210-12, respectively. In the preparation of S[D (Y-62)6]18, D(Y-62)6 was used as a starting material. Dealumination conditions for these zeolites are described elsewhere (*9*). For these series, the parent Y zeolite is indicated in parentheses. The number immediately following the brackets indicates framework Si/Al ratio. These were determined (*9a*) by ^{29}Se:MAS–NMR.

All zeolites were treated with 3.5 *M* ammonium acetate solution to remove residual Na^+. The slurry was heated for 2 h at reflux temperature with stirring and was then washed to remove soluble salts. Ion exchange was carried out three times. After final exchange, the catalysts were dried at 100°C to a freely flowing powder.

Instrument grade 10% i-butane in nitrogen, obtained from Matheson, was used as received. It contained 0.02% propane and 0.03% *n*-butane as impurities. Gold label 99.3% *n*-pentane with trace impurities of 0.4% i-pentane and 0.3% *n*-hexane was obtained from Aldrich. This *n*-pentane was stored over 5A molecular sieves in an inert atmosphere. Nitrogen obtained from Linde (99.999% purity, H_2O <3, total hydrocarbons <1, and O_2 <1 ppm) was used as a carrier gas for *n*-pentane.

Procedures

Cracking reactions were performed in a steady-state mode at atmospheric pressure. Aliquots of the zeolite catalysts (0.43- to 0.85-mm particle size) were selected for

testing. These were heated in an open quartz crucible at 400°C for 5 h. After covering with a lid, they were cooled to room temperature and 65 mg was transferred into an 8-mm-i.d. quartz U-tube reactor. The catalyst was held in place by quartz plugs on both the sides. A shallow catalyst bed was used (the bed length to diameter ratio was below 0.5). A thermocouple was positioned in the catalyst bed and the heating ramp was controlled by a Eurotherm Model 847 temperature controller. The heating rate used was less than 5 K/min and the maximum temperature used was 500°C. Otherwise thermal dealumination could be observed by ^{27}Al MAS–NMR. Flow rates of the gases were controlled by a Brooks mass flow controller units. Catalysts were pretreated at 400°C with oxygen and nitrogen for 2 h each before carrying out the reaction at 400°C. The pre- and postreaction zones were maintained at 100°C using heating tapes and ovens.

During *n*-pentane cracking, the carrier nitrogen was bubbled through a pool of *n*-pentane in a 30-cm-long saturator maintained at 25.0 ± 0.1°C by a Beckman thermocirculator. For both the reactants, the space velocity (F/W) was 1.1×10^{-5} mol reactant per gram of zeolite per second. The reaction was continued for 200 min under these conditions.

The analysis of the reaction products was performed by on-line GLC (TCD and FID). For isobutane, H_2 and CH_4 were determined using a TCD detector following a $\frac{1}{8}$ in. × 3 ft stainless-steel column packed with 5A molecular sieves at 0°C. Hydrocarbons (C_2 to C_6) were analyzed with an FID using an $\frac{1}{8}$ in. × 8 ft column containing in tandem dibenzylamine followed by propylene carbonate, both on Chromosorb, at 0°C. This allowed separation of ethane from ethene in the hydrocarbon analysis. For *n*-pentane, H_2 and CH_4 were determined using a similar column thermostated at 25°C and the hydrocarbons were analyzed by FID using a 30-ft-long $\frac{1}{8}$-in. stainless-steel column containing 23% SP-1700 on 80/100 mesh Chromosorb W at 70°C. Both GLC units were calibrated using pure gases up to C_6. In the FID analysis, 1-pentene appeared with neopentane, which was assumed to be negligible. The remaining five pentenes were separated from C_5 alkanes. Identification was made using retention times determined for authentic samples. Determination of H_2 was least accurate, but the figures given are correct to about $\pm 0.1 \times 10^{-9}$ mol/g s.

RESULTS

Treatment of Data

Differential conversion levels were maintained in all the activity measurements; i.e., the conversion was kept below 2.5% and usually around 1%. Under these conditions, the rate of formation of each product could be taken as $C_i = X_i(F/W)$ mol/g s, where X_i is the fractional conversion of isobutane to the ith product and F and W are respectively the corresponding flow rate and weight of the catalyst tested. Chain length A was defined as the ratio of rate of the propagation to the rate of the initiation reaction, i.e., the i-butane molecules reacted by H^- transfer in a bimolecular propagation to those reacted in the unimolecular initiation. Alternatively, chain length B is the ratio of the rates of propagation and termination, i.e., the number of times the carbenium ion chain propagates before it terminates leaving behind the original Brønsted acid site. In the steady state, both chain lengths A and B should be the same.

Conversion A was calculated by adding the rate of consumption of reactant in the unimolecular step (initiation) to the rate of consumption by H^- transfer to existing carbenium ions in a bimolecular step (propagation). Thus, these data are the sum of the rates of formation of hydrogen and alkanes. Conversions B and C were obtained based on the carbon and hydrogen balances over the products, respectively. Thus, the contributions of initiation, propagation, and termination steps were separated based on the Brønsted acid-catalyzed cracking mechanism of i-butane and *n*-pentane. This has

been explored previously (*4a*) for i-butane. It has been extended herein for *n*-pentane.

The possible contribution of thermal cracking was tested in an empty reactor. For both i-butane and *n*-pentane cracking, it was found to be less than 1% of the total conversion under typical reaction conditions and hence was neglected. Hexanes formed during *n*-pentane cracking are not shown in the final product distribution. Their contribution toward total conversion was negligible.

Activity Measurements

Conversions of i-butane decreased only slightly during the initial few minutes and then remained fairly constant over a remaining period of 200 min. Very little coke was formed during this reaction. For example, on S(LZ12)7 zeolite, 6 mg coke/g zeolite (H/C = 1.3) was generated. This is equivalent to only 0.19 carbon atoms/Al_t atom. Since many carbon atoms are present wherever a coke deposit exists, evidently only a very small percentage of the total sites was affected.

Activity data for i-butane cracking as a function of lattice aluminum content taken as lattice Al_t–Na^+ over HY zeolites are shown in Fig. 1A. They resemble those of previous reports for *n*-hexane (*10*), but are somewhat better defined. Similar results for steamed catalysts were also obtained. Two distinct volcano type activity patterns were observed. One was composed of structurally pure LZY (commercial) and DY (AHS treated) zeolites. The other was constituted from the data for SY (steamed) zeolites, which contain large quantities of extralattice alumina. The maxima obtained for LZY and DY zeolites were close to 17×10^{20} Al atoms/g (32 Al atoms/uc), as reported by Lunsford and co-workers (*10*). The second maximum for SY zeolites appeared at lower lattice aluminum concentration, i.e., about 8×10^{20} Al atoms/g. These data were obtained, starting with LZY-210(12), by steaming aliquots under successively more severe conditions to effect increasing extents of dealumination. The point for LZY-82 did not fit with the rest of the data although the substantial activity enhancement obtained by steaming is quite evident. This was not surprising since the preparation history (dealumination conditions and starting material) for LZY-82 was totally different from other SY zeolites. Interestingly, in agreement with the data of Lago *et al.* (*11*) for HZSM-5 zeolites, the SY zeolites were found to be more active than the DY and LZY zeolites.

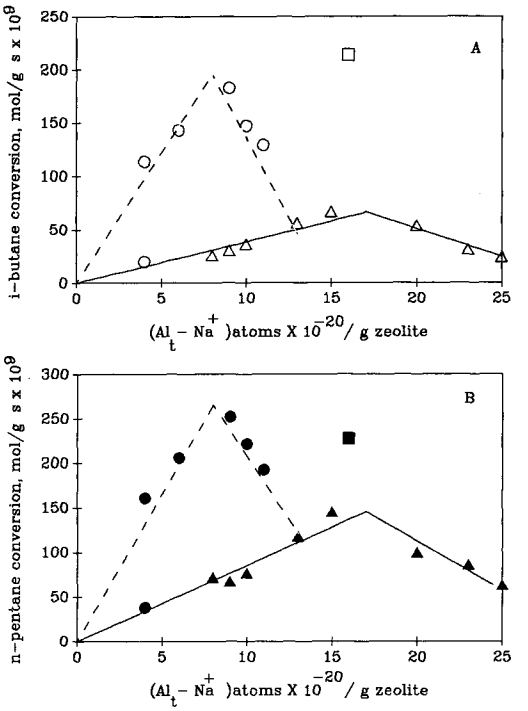

FIG. 1. (A) Conversion of i-butane (open symbols) and (B) *n*-pentane (solid symbols) as a function of lattice aluminum content. In each case, the catalyst weight was 65 mg, F/W was 1.1×10^{-5} mol/g s, reaction temperature was 400°C, and time on stream was 200 min. (△, ▲) Ammonium hexafluorosilicate-treated HY zeolites; (○, ●) the steamed HY zeolites, except for LZY-82 (□, ■).

The activities for *n*-pentane cracking on the same S, D, and LZY zeolites, as a function of lattice aluminum content, are shown in Fig. 1B. Note the striking similarity between the activity patterns obtained for i-butane and *n*-pentane cracking. The same

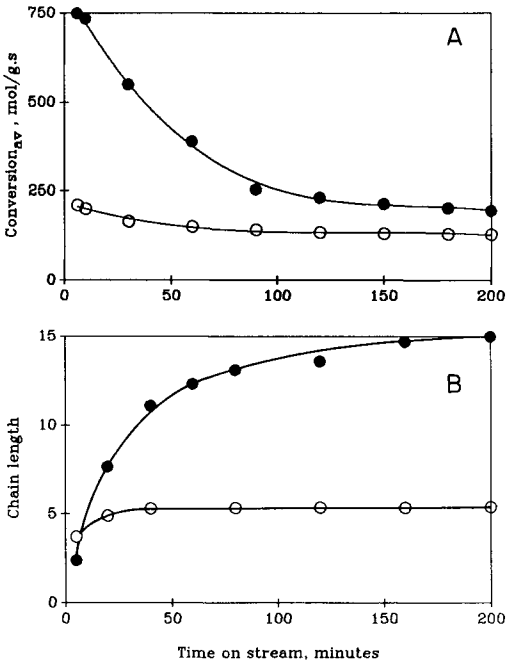

FIG. 2. (A) Variation in conversion and (B) chain length with time on-stream over S(LZ-12)7 zeolite. (○) i-Butane cracking; (●) *n*-pentane cracking. Catalyst loading was 65 mg, *F/W* was 1.1×10^{-5} mol/g s, and reaction temperature was 400°C. Data were collected under identical conditions for the two reactions studied.

two volcano type curves appeared for D and LZY zeolites and for SY zeolites, respectively. The lattice aluminum content at which the maximum activity was reached for *n*-pentane cracking was identical to that for i-butane cracking, for both sets of zeolites.

As shown in Fig. 2A, the activity for *n*-pentane cracking decreased slowly, but continuously with time. The data listed in the tables were taken at 200 min where the decrease in reaction rate was less than 5×10^{-9} mol/g h. The amount of coke generated after 200 min during *n*-pentane cracking over S(LZ-12)7 was about 79 mg coke/g zeolite (H/C = 1.1). This is equivalent to 2.6 carbon atoms/Al$_t$ atom, i.e., more than 10-fold larger than with i-butane. As reported previously (*4a, 7*), i-butane cracking was clean and the catalyst activity did not vary significantly with time on stream.

Mechanistic Studies

Selectivity data and some properties calculated therefrom for i-butane and *n*-pentane cracking on different D, LZ, and SY zeolites are given in Tables 1 through 8. In all cases, there was good agreement between the conversion rates obtained by Schemes A, B, and C.

The data for isobutane cracking over all the catalysts followed a similar pattern. The chief products were *n*-butane, propane, and i-butene, accompanied by smaller but comparable amounts of CH_4 and H_2. The rate of CH_4 production was higher, sometimes almost twice as high as the rate of H_2 formation. Significant amounts of isopentane and other alkanes were also present. The gross data show that the hydrogen has been redistributed from isobutane to methane and propane, together with the formation of i-butene. This process is far from stoichiometric, however; the reasons for this will become clear when the details of the mechanism are discussed in a later section of this paper. Similarly more C_3 products were generated than can be accounted for by the two known direct pathways, viz., together with CH_4 in the initiation step and together with isopentane during disproportionation (to be discussed in a later paper.)

During *n*-pentane cracking, hydrogen and 1-pentene were detected only for the first few minutes of the reaction. The reaction was initiated mainly by the attack of Brønsted acid protons on C–C bonds generating CH_4 and C_2H_6 as the products of initiation. The rate of formation of C_2H_6 was almost twice the rate of formation of CH_4. Isomerization selectivity for i-pentane formation was around 75%. Presumably this resulted from the chain propagation step, vide infra. Among the other alkanes, isobutane and propane were major products. The quantity of C_4 alkanes was higher than could be accounted for by CH_4 and the hexanes that appeared in trace amounts.

TABLE 1

Rates of Product Formation and Reaction of Isobutane on D and LZY Zeolites

Catalyst:	LZY-62	D(Y-62)3	LZ-210-6	LZ-210-9
Si/Al:	2.5	2.9	3.4	5.0
$(Al_t–Na^+)$ atom $\times 10^{-20}$/g:	25	23	20	15
Product mol/g s $\times 10^9$				
Hydrogen	1.8	2.3	3.7	4.9
Methane	1.9	4.5	6.6	8.6
Ethane	0.5	0.4	0.5	0.8
Ethene	0	0	0	0.2
Propane	10.5	11.1	15.1	18.1
Propene	0.6	1.9	7.7	5.2
i-Butane	R	R	R	R
n-Butane	9.4	11.0	22.2	27.6
1-Butene	0.1	0.1	1	1.6
i-Butene	5.1	7.9	7.3	9.7
2-Butene (*cis, trans*)	0	0	0.4	1.0
1-3-Butadiene	0	0	0	0
i-Pentane	1.1	1.8	4.0	8.9
n-Pentane	0	0	0	0
1-Pentene + neopentane	0	0	0	0
2-Pentene + *i*-pentene	0	0	0	0
Initiation	3.7	6.7	10.4	13.5
Propagation	21.5	24.4	41.9	55.5
Termination	5.8	9.9	16.4	17.7
Conversion A	25.2	31.1	52.3	69
Conversion B	25.0	32.4	55.0	71.3
Conversion C	25.0	32.1	54.4	70.8
% Conversion	0.23	0.28	0.49	0.64
Chain length A	5.8	3.7	4.0	4.1
Chain length B	3.7	2.5	2.6	3.1

Note. Rates are given as 10^9 mol/g s; catalyst loading was 0.065 g; F/W was 1.1×10^{-5} mol/g s; reaction temperature was 400°C; time on stream was 200 min. Initiation = $H_2 + CH_4$; propagation = $\Sigma_2^5 C_nH_{2n+2}$; termination = $\Sigma_2^4 C_nH_{2n}$. Conversion A = $H_2 + CH_4 + \Sigma_2^5 C_nH_{2n+2}$. Conversion B = $(\frac{1}{4}) \Sigma_1^5 jC_j$, where j is the number of carbon atoms in the ith product. Conversion C = $(\frac{1}{16}) \Sigma_0^5 jH_j$, where j is the number of hydrogen atoms in the ith product. % Conversion = average of percentage conversion A, B, C. Chain length A = propagation/initiation; chain length B = propagation/termination.

As with i-butane cracking, the chain termination steps should involve formation of alkenes. This was substantiated by the reasonable agreement of the rates of initiation and termination calculated on this basis. Propene and smaller amounts of other alkenes such as the butenes, 2-pentene, and i-pentene were formed together with small quantities of butadiene. In the steady state, hydrogen, 1-pentene, and neopentane were not observed with any of the catalysts. In many cases, Conversion A was found to be about 5% higher than Conversion B, suggesting that significant amounts of hydrocarbons were left behind as coke.

DISCUSSION

Cracking of i-butane has been modeled (*4a, 7, 12*) as a carbenium ion chain reaction, initiated by protonation of isobutane and resulting in the formation of CH_4 and H_2, together with the corresponding carbenium ions. Thus, the rate of chain initiation may be taken as the sum of the rates of formation

TABLE 2

Rates of Product Formation and Reaction of Isobutane on D and LZY Zeolites

Catalyst:	LZ-210-12	D(Y-62)6	D(Y-62)7	D(Y-62)8
Si/Al:	6	6.5	7	7.5
$(Al_t\text{–}Na^+)$ atoms $\times 10^{-20}$/g:	13	10	9	8
Product mol/g s $\times 10^9$				
Hydrogen	3.6	2.4	2.2	2
Methane	4.3	3.0	2.6	2.3
Ethane	0.7	0.5	0.4	0.4
Ethene	0.2	0.1	0	0
Propane	14.1	12.2	10.7	10.1
Propene	2.5	2.6	2.0	1.7
i-Butane	R	R	R	R
n-Butane	19.1	14.9	11.8	10.8
1-Butene	1.1	0.2	0	0
i-Butene	6.3	8.3	7.6	6.9
2-Butene (*cis, trans*)	0.5	0	0	0
1-3-Butadiene	0	0	0	0
i-Pentane	4.7	1.1	0.8	0.8
n-Pentane	0	0	0	0
1-Pentene + neopentane	0	0	0	0
2-Pentene + *i*-pentene	0	0	0	0
Initiation	8	5.4	4.8	4.3
Propagation	38.7	28.7	23.8	22.1
Termination	10.4	11.1	9.6	8.6
Conversion A	46.6	34.1	28.5	26.4
Conversion B	46.8	36.8	30.8	28.3
Conversion C	46.8	36.3	30.4	27.9
% Conversion	0.42	0.33	0.28	0.25
Chain length A	4.8	5.3	4.9	5.1
Chain length B	3.7	2.6	2.5	2.6

Note. Rates are given as 10^9 mol/g s; catalyst loading was 0.065 g; F/W was 1.1×10^{-5} mol/g s; reaction temperature was 400°C; time on stream was 200 min. Initiation = $H_2 + CH_4$; propagation = $\Sigma_2^5 C_nH_{2n+2}$; termination = $\Sigma_2^4 C_nH_{2n}$. Conversion A = $H_2 + CH_4 + \Sigma_2^5 C_nH_{2n+2}$. Conversion B = $(\frac{1}{4})\Sigma_1^5 jC_j$, where j is the number of carbon atoms in the ith product. Conversion C = $(\frac{1}{10})\Sigma_0^5 jH_j$, where j is the number of hydrogen atoms in the ith product. % Conversion = average of percentage conversion A, B, C. Chain length A = propagation/initiation; chain length B = propagation/termination.

of CH_4 and H_2. When the overall rate of reaction (average of Conversions A, B, and C) was plotted against the rate of initiation (Fig. 3) linear correlations resulted as expected at low conversion for this model. On the other hand plots of chain length vs overall rate were found to be constant, within the experimental error, for each catalyst type (Fig. 4). These nearly constant values increased somewhat with the increasing slopes of Fig. 3, suggesting that different pretreatments generated sites of varying intensive factor of acidity.

As shown in Figs. 3 and 4, similar results were obtained for *n*-pentane cracking. Modeling the rate of chain initiation as the sum of rates of formation of CH_4 and C_2H_6, linear relationships between the rate of reaction and the rate of initiation were obtained. The slope of these lines is an approximate measure of the average chain length A. The values so deduced were: i-butane on DY and

TABLE 3

Rates of Product Formation and Reaction of Isobutane on SY Zeolites

Catalyst:	LZY-82	S(LZ-12)7	S(LZ-12)8	S(LZ-12)10
Si/Al:	5.1	7.3	8.3	9.7
$(Al_t–Na^+)$ atoms $\times 10^{-20}$/g:	16	11	10	9
Product mol/g s $\times 10^9$				
Hydrogen	9.4	7.2	7.7	10.6
Methane	15.7	12	14	16.8
Ethane	1.6	0.7	0.9	2.6
Ethene	0.4	0.1	0.1	0.7
Propane	47	30.5	34.5	32.9
Propene	8.1	4.7	5.4	11.9
i-Butane	R	R	R	R
n-Butane	102.7	64.9	73.1	72.2
1-Butene	3.2	1.9	3	2.8
i-Butene	16.5	11.9	11.9	19.1
2-Butene (*cis, trans*)	3.4	1.9	2.9	1.4
1-3-Butadiene	0	0	0	0
i-Pentane	34.3	15	18	36.1
n-Pentane	0	0	0	2.4
1-Pentene + neopentane	0	0	0	0
2-Pentene + *i*-pentene	0	0	0	0
Initiation	25.1	19.2	21.7	27.4
Propagation	185.6	111	126.6	146.1
Termination	31.2	20.4	23.2	35.3
Conversion A	210.6	130.2	148.3	173.5
Conversion B	214.7	129.1	147.3	182.7
Conversion C	214.1	129.4	147.6	181.1
% Conversion	1.9	1.2	1.3	1.6
Chain length A	7.4	5.8	5.8	5.3
Chain length B	5.9	5.4	5.5	4.1

Note. Rates are given as 10^9 mol/g s; catalyst loading was 0.065 g; F/W was 1.1×10^{-5} mol/g s; reaction temperature was 400°C; time on stream was 200 min. Initiation = $H_2 + CH_4$; propagation = $\sum_2^5 C_nH_{2n+2}$; termination = $\sum_2^4 C_nH_{2n}$. Conversion A = $H_2 + CH_4 + \sum_2^5 C_nH_{2n+2}$. Conversion B = $(\frac{1}{4}) \sum_1^5 jC_i$, where j is the number of carbon atoms in the ith product. Conversion C = $(\frac{1}{10}) \sum_0^5 jH_i$, where j is the number of hydrogen atoms in the ith product. % Conversion = average of percentage conversion A, B, C. Chain length A = propagation/initiation; chain length B = propagation/termination.

LZY, 4; i-butane on SY, 7; *n*-pentane on DY and LZY, 8; *n*-pentane on SY, 15. These values are in reasonable agreement with those shown in Fig. 4. The points for LZY-82(squares) do not fit well with the remainder of the data, but appear to best conform to the data for the steamed catalysts.

Chain lengths increased with time on stream for both the substrates. For i-butane this was small and took place over the first 25 min. For *n*-pentane the increase was much larger and continuous. This is depicted for catalyst S(LZ-12)7 in Fig. 2B, which is typical for all the catalysts. The increase in chain length for i-butane cracking was negligible, whereas for *n*-pentane cracking it was substantial. It corresponded to a 10-fold decrease in the initiation rate while the propagation rate decreased by only a factor of about three. On the lined out catalysts, chain lengths did not change significantly even when the temperature was varied from 350 to 450°C.

Overall activity trends on these zeolites

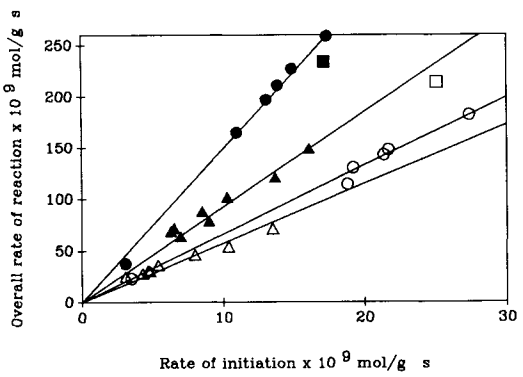

FIG. 3. Dependence of the total rate on the rate of initiation for the two reactions. (△) i-Butane, D and LZY; (▲) *n*-pentane, D and LZY; (○) i-butane, SY; (●) *n*-pentane, SY; (□ and ■) LZY-82 for these two reactions.

were similar for both the reactions (Figs. 1 and 2) and were found to be dependent on the amounts of lattice and extralattice alumina, as reported by others (*2, 5, 7, 9–13*). For DY and LZY zeolites, a volcano type relationship between activity and the amount of lattice alumina was observed in agreement with the data of Sohn *et al.* (*10*), who have argued that this volcano type curve is caused by opposing effects of increasing numbers and decreasing strengths of lattice acid sites as the lattice aluminum content is increased to the point where second nearest neighbor interactions set in. For SY zeolites, the activity is increased over that of the parent catalyst and that expected based on the lattice aluminum content. Lago *et al.* (*11*) have suggested that this increase in activity is due to a Brønsted acid–Lewis acid interaction, which is somehow developed between lattice and extralattice alumina. More generally it could be said that it reflects a poorly understood lattice reconstruction.

It is interesting that the *n*-pentane reaction can be analyzed using the same model used for i-butane with only slight modification. This supports the concept of common chemistry for these small alkanes, viz., carbenium ion chains initiated by protonation of the substrate. These data will serve as a bridge to the widely used, but more complicated, *n*-hexane cracking reaction (*5, 6, 10*). It is also interesting that no hydrogen was formed during cracking of *n*-pentane, which contains secondary but no tertiary hydrogens, yet alkane formation was facile.[1]

The following kinetic picture explains most of our results. The kinetic modeling was made possible by using simple molecules that cannot undergo β-scission and by using very low conversions so that hydride transfer occurs exclusively from the reactant to the various carbenium ions generated on the surface. With larger molecules or with higher conversions, these same processes will be occurring, but the picture will be clouded by additional or by secondary processes.

Initiation. The chain is initiated by indirect formation of the chain carrying carbenium ions. With i-butane, these reactions are

$$(CH_3)_3CH + H^+ \rightarrow CH_3{-}\overset{\displaystyle CH_3}{\overset{|}{\underset{\displaystyle CH_3}{\overset{|}{C^+}}}}\!\!<\!\!\begin{matrix}H\\H\end{matrix} \qquad (1)$$

$$\rightarrow H_2 + t{-}C_4H_9^+$$
$$\rightarrow CH_4 + \text{sec}{-}C_3H_7^+.$$

Both CH_4 and H_2 are stable; they will not react further. So the rate of initiation can be taken as the sum of their rates of formation.

With *n*-pentane, no H_2 was produced; hence no C_5 carbenium ions can be formed in the initiation step. Instead of protonolysis of C–H bonds, C–C bonds are attacked. This results in the formation of CH_4 and C_2H_6, together with C_4^+ and C_3^+ carbenium

[1] *Note added in proof.* Kannila et al. (*4c*) have very recently reported that H_2 is produced during the cracking of *n*-butane over HZSM-5. We have confirmed this finding over several of the catalysts reported herein.

TABLE 4

Rates of Product Formation and Reaction of Isobutane on SY Zeolites

Catalyst:	S(LZ-12)14	S(LZ-12)18	S(D(Y-62)6)18
Si/Al:	14.1	17.6	18
(Al_f–Na^+) atoms × 10^{-20}/g:	6	4	4
Product mol/g s × 10^9			
Hydrogen	10	7.1	1.7
Methane	11.4	11.8	1.9
Ethane	1.1	1.2	0.3
Ethene	0.1	0.1	0
Propane	30.9	35.4	8.8
Propene	7.2	4.7	1.4
i-Butane	R	R	R
n-Butane	61.8	57	9
1-Butene	3.4	4	0
i-Butene	14.6	14.3	5.6
2-Butene (*cis, trans*)	1.9	0.2	0.6
1-3-Butadiene	0	0	0
i-Pentane	23.7	3.7	0
n-Pentane	0	0	0
1-Pentene + neopentane	0	0	0
2-Pentene + *i*-pentene	0	0	0
Initiation	21.4	18.8	3.5
Propagation	117.5	97.2	18.2
Termination	27.1	23.2	7.7
Conversion A	139	116.1	21.7
Conversion B	143.3	113.7	23.6
Conversion C	142.6	114.3	23.2
% Conversion	1.3	1	0.2
Chain length A	5.4	5.1	5.2
Chain length B	4.3	4.2	2.4

Note. Rates are given as 10^9 mol/g s; catalyst loading was 0.065 g; *F/W* was 1.1 × 10^{-5} mol/g s; reaction temperature was 400°C; time on stream was 200 min. Initiation = $H_2 + CH_4$; propagation = $\Sigma_2^5 C_nH_{2n+2}$; termination = $\Sigma_2^4 C_nH_{2n}$. Conversion A = $H_2 + CH_4 + \Sigma_2^5 C_nH_{2n+2}$. Conversion B = $(\frac{1}{4})\Sigma_1^5 jC_i$, where j is the number of carbon atoms in the ith product. Conversion C = $(\frac{1}{10})\Sigma_0^5 jH_i$, where j is the number of hydrogen atoms in the ith product. % Conversion = average of percentage conversion A, B, C. Chain length A = propagation/initiation; chain length B = propagation/termination.

ions, respectively. Hence, the initiation reactions are

$$CH_3CH_2CH_2CH_2CH_3 + H^+ \rightarrow$$

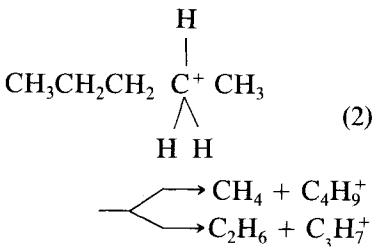

$$\rightarrow CH_4 + C_4H_9^+$$
$$\rightarrow C_2H_6 + C_3H_7^+ \qquad (2)$$

and

$$CH_3CH_2CH_2CH_2CH_3 + H^+ \rightarrow$$

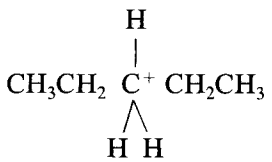

$$C_2H_6 + C_3H_7^+. \qquad (3)$$

It may be supposed that although primary carbenium ions would be released, these un-

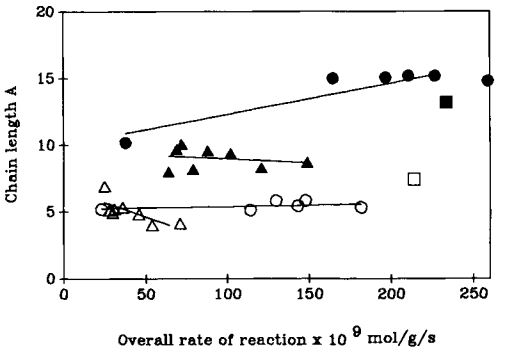

FIG. 4. Relationship between the chain length A and total rate. (△) i-Butane D and LZY; (▲) n-pentane, D and LZY; (○) i-butane, SY; (●) n-pentane, SY; (□ and ■) LZY-82 for these same two reactions.

dergo a concerted rearrangement into the more stable secondary carbenium ions via a H^- shift. Thus, the rates of chain initiation given in Tables 5–8 are taken as the sum of the rates of formation of CH_4 and C_2H_6. Note that without chain carrying steps, no C_5 products would be produced.

Propagation. Carbenium ion chains are propagated by a set of reactions that first consume the carbenium ions formed in the initiation step and then regenerate them from the reactant. With i-butane, these reactions are

$$t\text{—}C_4H_9^+ \rightleftharpoons \underline{\text{sec—}C_4H_9^+} \qquad (4)$$

followed by

$$\text{sec—}C_4H_9^+ + \text{i—}C_4H_{10} \rightarrow n\text{—}C_4H_{10} + \underline{\text{t—}C_4H_9^+} \qquad (5)$$

and

$$\text{sec—}C_3H_7^+ + \text{i—}C_4H_{10} \rightarrow \underline{t\text{—}C_4H_9^+} + C_3H_8. \qquad (6)$$

Note that H^- transfer from i-butane to t—$C_4H_9^+$ is degenerate so that the isomerization step is necessary. The original t—$C_4H_9^+$ is regenerated according to Eq. (5). Reactions (4) and (5) may go on continuously until interrupted by loss of the chain carrier by an alternative process, e.g., desorption of an olefin.

With n-pentane, the sec—$C_3H_7^+$ and sec—$C_4H_9^+$ produced in the initiation step must undergo hydride transfer with the substrate forming the sec—$C_5H_{11}^+$ ion, which becomes a chain carrier, i.e.,

$$\text{sec—}C_3H_7^+ + n\text{—}C_5H_{12} \rightarrow C_3H_8 + \underline{\text{sec—}C_5H_{11}^+} \qquad (7)$$

$$\text{sec—}C_4H_9^+ + n\text{—}C_5H_{12} \rightarrow n\text{—}C_4H_{10} + \underline{\text{sec—}C_5H_{11}^+} \qquad (8)$$

$$\text{sec—}C_4H_9^+ \rightarrow \underline{t\text{—}C_4H_9^+} \qquad (9)$$

$$t\text{—}C_4H_9^+ + n\text{—}C_5H_{12} \rightarrow \text{i—}C_4H_{10} + \underline{\text{sec—}C_5H_{11}^+} \qquad (10)$$

$$\text{sec—}C_5H_{11}^+ \rightleftharpoons \underline{t\text{—}C_5H_{11}^+} \qquad (11)$$

$$t\text{—}C_5H_{11}^+ + n\text{—}C_5H_{12} \rightarrow \text{i—}C_5H_{12} + \underline{\text{sec—}C_5H_{11}^+}. \qquad (12)$$

Reactions (11) and (12) go on continuously until the sec—$C_5H_{11}^+$ is lost by an alternative process. As in isobutane cracking, isomerization plays a key role, and thus i-pentane becomes a major product.

Termination. The chain reactions terminate by the decomposition of carbenium ions into alkenes, thus regenerating the original Brønsted acid sites. Alkenes from C_2 to C_5 were observed. Note the agreement between the rates of initiation and termination calculated in this way. These compounds can readily participate in oligomerization reactions leading to secondary chemistry involving rearrangement by isomerization, intramolecular H^- transfer, and β-scission. These reactions distort the picture at higher conversions.

Carbenium ions are continuously being produced by the chemistry described above. In the steady state these processes are balanced by desorption, i.e.,

$$C_nH_{2n+1}^+Z^- \overset{K}{\rightleftharpoons} C_nH_{2n} + HZ. \qquad (13)$$

Several points are apparent here. (a) Each olefin should have a different equilibrium constant, with larger branched tertiary ions being more stable than smaller secondary or

TABLE 5

Rates of Product Formation and Reaction of *n*-Pentane on D and LZY Zeolites

Catalyst:	LZY-62	D(Y-62)3	LZ-210-6	LZ-210-9
Si/Al:	2.5	2.9	3.4	5.0
$(Al_f\text{–}Na^+)$ atoms $\times 10^{-20}$/g:	25	23	20	15
Product mol/g s $\times 10^9$				
Hydrogen	0	0	0	0
Methane	2.2	2.7	3.2	4.5
Ethane	4.8	5.8	7.1	11.6
Ethene	0.3	0.5	0.8	1
Propane	3.3	5.5	8.1	13.3
Propene	5.5	5.2	5	8.6
i-Butane	4.7	7.1	8.8	17.7
n-Butane	1.4	2.1	3.1	5
1-Butene	2.4	1.9	1.7	2.7
i-Butene	1	0.8	0.7	1.2
2-Butene (*cis, trans*)	0.6	0.4	0.5	0.8
1-3-Butadiene	1.4	0	0	0
i-Pentane	47	67.1	76.7	108
n-Pentane	R	R	R	R
1-Pentene + neopentane	0	0	0	0
2-Pentene + *i*-pentene	0.9	1.1	2	2.2
Initiation	7	8.5	10.3	16.1
Propagation	56.3	81.8	96.7	140
Termination	11.7	9.4	9.8	15.5
Conversion A	63.3	90.3	107	156.1
Conversion B	64.6	87.3	102	147.6
Conversion C	64.1	88	102.8	149.1
% Conversion	0.6	0.78	0.91	1.3
Chain length A	8	9.6	9.4	8.7
Chain length B	4.8	8.7	9.9	9

Note. Rates are given as 10^9 mol/g s; catalyst loading was 0.065 g; *F/W* was 1.1×10^{-5} mol/g s; reaction temperature was 400°C; time on stream was 200 min. Initiation = $H_2 + CH_4 + C_2H_6$; propagation = $\Sigma_3^5 C_nH_{2n+2}$; termination = $\Sigma_2^5 C_nH_{2n}$. Conversion A = $H_2 + CH_4 + C_2H_6 + \Sigma_3^5 C_nH_{2n+2}$. Conversion B = $(\frac{1}{5}) \Sigma_1^5 jC_i$, where j is the number of carbon atoms in the ith product. Conversion C = $(\frac{1}{12}) \Sigma_0^5 jH_i$, where j is the number of hydrogen atoms in the ith product. % Conversion = average of percentage conversion A, B, C. Chain length A = propagation/initiation; chain length B = propagation/termination.

primary ions. (b) These equilibrium constants should reflect the stabilizing influence of the conjugate base (Z^-); this is dependent on the delocalization volume (*14–16*) available for the extra charge put on the lattice on formation of the carbenium ion [it is the shrinkage of this volume that effects the decreasing activity at aluminum concentrations above about 32 Al/u.c. (*10*)] and it is an important part of the intensive factor of the acidity (*14–16*). (c) Since under reaction conditions K will be large, desorption and olefin formation must be keenly competitive with formation of paraffins. (d) Thus the lifetime of the carbenium ion may limit the extent of the bimolecular hydride transfer reaction. And (e) the ease with which desorbed olefins can be readsorbed as they diffuse out of the pore system and escape the bed will tend to govern the chain length. Catalyst acidity, as expressed by Eq. (13), depends not only on the proton donating ability of the site, but on the ability of the lattice to stabilize the carbenium ion. That

TABLE 6

Rates of Product Formation and Reaction of *n*-Pentane on D and LZY Zeolites

Catalyst:	LZ-210-12	D(Y-62)6	D(Y-62)7	D(Y-62)8
Si/Al:	6	6.5	7	7.5
(Al_t–Na^+) atoms × 10^{-20}/g:	13	10	9	8
Product mol/g s × 10^9				
Hydrogen	0	0	0	0
Methane	3.5	2.5	2.1	2.1
Ethane	10.2	6.5	4.1	4.4
Ethene	0.6	0.5	0.3	0.3
Propane	11.5	7.2	3	3.3
Propene	7.6	4.4	5.4	5
i-Butane	11.8	7.4	5.2	5
n-Butane	4.4	2.8	1.4	1.9
1-Butene	2.3	1.7	2.1	2.1
i-Butene	1	0.7	0.9	0.8
2-Butene (*cis, trans*)	0.7	0.3	0.6	0.5
1-3-Butadiene	0	0	0	1.5
i-Pentane	85.4	56.7	51.3	55.3
n-Pentane	R	R	R	R
1-Pentene + neopentane	0	0	0	0
2-Pentene + *i*-pentene	2.1	1.7	1	0.8
Initiation	13.7	9	6.3	6.5
Propagation	113.2	74	61	65.5
Termination	13.7	8.8	12	10.7
Conversion A	126.9	83	67.2	72
Conversion B	120	78.7	69.3	72.7
Conversion C	121.3	79.5	68.8	72.3
% Conversion	1.1	0.7	0.6	0.65
Chain length A	8.3	8.2	9.7	10.1
Chain length B	8.3	8.4	5.1	6.1

Note. Rates are given as 10^9 mol/g s; catalyst loading was 0.065 g; F/W was 1.1×10^{-5} mol/g s; reaction temperature was 400°C; time on stream was 200 min. Initiation = $H_2 + CH_4 + C_2H_6$; propagation = $\Sigma_3^5 C_nH_{2n+2}$; termination = $\Sigma_2^5 C_nH_{2n}$. Conversion A = $H_2 + CH_4 + C_2H_6 + \Sigma_3^5 C_nH_{2n+2}$. Conversion B = $(\frac{1}{5})\ \Sigma_1^5 jC_j$, where j is the number of carbon atoms in the ith product. Conversion C = $(\frac{1}{12})\ \Sigma_0^5 jH_i$, where j is the number of hydrogen atoms in the ith product. % Conversion = average of percentage conversion A, B, C. Chain length A = propagation/initiation; chain length B = propagation/termination.

this is so can readily be seen when alkane to alkene ratios obtained over mordenites, or on the other hand silica–alumina cracking catalysts, are compared with those over Y zeolites. The much longer chain lengths obtained with the former (*2*) result from the higher steady-state concentrations of carbenium ions on the surface. The reverse is true with silica–alumina (*2*).

In the present work, changes in activity with both composition and pretreatment (steaming) are clearly evident. These changes may be supposed to reflect the acidity of the preparations. The data of Fig. 3 show that the overall rate of conversion varied linearly with the rate of initiation. In these experiments variation in chain length was relatively small, although the effects of steaming were clearly evident, especially with *n*-pentane. These results suggest that the intensive factor of the acidity remains fairly constant as Al sites are replaced with Si, but is enhanced by steaming.

The reaction chemistry described above

TABLE 7

Rates of Product Formation and Reaction of *n*-Pentane on SY Zeolites

Catalyst:	LZY-82	S(LZ-12)7	S(LZ-12)8	S(LZ-12)10
Si/Al:	5.1	7.3	8.3	9.7
$(Al_t\text{–}Na^+)$ atoms $\times 10^{-20}$/g:	16	11	10	9
Product mol/g s $\times 10^9$				
Hydrogen	0	0	0	0
Methane	4.5	5.2	5.8	6.5
Ethane	12.6	7.9	9.1	10.9
Ethene	0.8	0.6	0.7	0.8
Propane	19.3	25.2	28.1	31.4
Propene	8.5	7.2	8.1	9
i-Butane	20.4	22.1	24.7	27.4
n-Butane	7.5	9.2	10.3	11.5
1-Butene	2.8	2.17	2.4	2.7
i-Butene	1.2	0.9	1	1.1
2-Butene (*cis, trans*)	0.77	0.6	0.6	0.7
1-3-Butadiene	0	0	0	0
i-Pentane	179.6	140.8	163.9	187.6
n-Pentane	R	R	R	R
1-Pentene + neopentane	0	0	0	0
2-Pentene + *i*-pentene	3.4	2.3	2.5	3.7
Initiation	17.2	13.1	14.9	17.4
Propagation	226.9	197.3	227	257.9
Termination	16.6	13.2	14.7	17.3
Conversion A	244	210.5	241.9	275.3
Conversion B	231.8	194.8	224.2	256
Conversion C	234.2	197.6	227.4	259.6
% Conversion	2.08	1.75	2.02	2.3
Chain length A	13.2	15.1	15.2	14.8
Chain length B	13.7	15	15.4	14.9

Note. Rates are given as 10^9 mol/g s; catalyst loading was 0.065 g; F/W was 1.1×10^{-5} mol/g s; reaction temperature was 400°C; time on stream was 200 min. Initiation = $H_2 + CH_4 + C_2H_6$; propagation = $\sum_3^5 C_nH_{2n+2}$; termination = $\sum_2^5 C_nH_{2n}$. Conversion A = $H_2 + CH_4 + C_2H_6 + \sum_3^5 C_nH_{2n+2}$. Conversion B = $(\frac{1}{5}) \sum_1^5 jC_i$, where j is the number of carbon atoms in the ith product. Conversion C = $(\frac{1}{12}) \sum_0^5 jH_i$, where j is the number of hydrogen atoms in the ith product. % Conversion = average of percentage conversion A, B, C. Chain length A = propagation/initiation; chain length B = propagation/termination.

is in general agreement with the data. In i-butane cracking, *n*-butane produced in the chain carrying reactions, was the largest single product. However, propane production was considerably larger than could be accounted for by disproportionation of two C_4 into C_3 and C_5 plus that resulting from Eq. (1) followed by (6). Evidently even at these low conversions secondary chemistry is apparent. This was limited, however, because the overall mass balances based on the simple picture (Conversions A) were in fair agreement with the cabon and the hydrogen balances (Conversions B and C). Isobutene was the chief termination product, as might be reasonably expected from the proposed reaction network. The sum of the alkenes formed (tabulated as a termination rate) was generally greater than the corresponding rate of initiation. These features were not observed, or at least were not so pronounced, in earlier work carried out at 370°C using 400 mg catalyst instead of 400°C and 65 mg catalyst. Several possible sources of

TABLE 8

Rates of Product Formation and Reaction of *n*-Pentane on SY Zeolites

Catalyst:	S(LZ-12)14	S(LZ-12)18	S(D(Y-62)6)18
Si/Al:	14.1	17.6	18
$(Al_f\text{–}Na^+)$ atoms $\times 10^{-20}$/g:	6	4	4
Product mol/g s $\times 10^9$			
Hydrogen	0	0	0
Methane	5.5	4.2	0.8
Ethane	8.4	6.7	2.3
Ethene	0.6	0.4	0
Propane	26.9	21.9	1.3
Propene	7.6	6.3	4.3
i-Butane	23.4	19.2	2.4
n-Butane	9.8	8	0.6
1-Butene	2.3	1.9	2.8
i-Butene	1	0.8	0.8
2-Butene (*cis, trans*)	0.9	0.5	0.5
1-3-Butadiene	0	0	1.4
i-Pentane	151	116	27.3
n-Pentane	R	R	R
1-Pentene + neopentane	0	0	0
2-Pentene + *i*-pentene	2.1	1.8	0.2
Initiation	13.9	11	3.1
Propagation	211.2	165.1	31.6
Termination	13.9	11.2	9.9
Conversion A	225.1	176.1	34.7
Conversion B	208.2	162.6	38.7
Conversion C	211.2	165	37.8
% Conversion	1.88	1.46	0.35
Chain length A	15.2	15	10.2
Chain length B	15.2	14.7	3.2

Note. Rates are given as 10^9 mol/g s; catalyst loading was 0.065 g; F/W was 1.1×10^{-5} mol/g s; reaction temperature was 400°C; time on stream was 200 min. Initiation = $H_2 + CH_4 + C_2H_6$; propagation = $\sum_3^5 C_nH_{2n+2}$; termination = $\sum_2^5 C_nH_{2n}$. Conversion A = $H_2 + CH_4 + C_2H_6 + \sum_3^5 C_nH_{2n+2}$. Conversion B = $(\frac{1}{5}) \sum_1^5 jC_j$, where j is the number of carbon atoms in the ith product. Conversion C = $(\frac{1}{12}) \sum_0^5 jH_i$, where j is the number of hydrogen atoms in the ith product. % Conversion = average of percentage conversion A, B, C. Chain length A = propagation/initiation; chain length B = propagation/termination.

these discrepancies are: (a) involvement of surface residues (H/C = 1.1–1.3), which are known to pass hydrogen into paraffinic products and which at very low conversions could distort the termination rates; (b) loss of H_2 from the analysis; and (c) other secondary oligomerization–cracking processes.

With *n*-pentane cracking, the agreement with the model was a bit better. Isopentane was in all cases the largest single product. Still, more butanes and propanes were produced than could be accounted for by the $CH_4 + C_2H_6$ formed in the initiation reaction. Again Conversions A, B, and C were in good agreement showing that the overall mass balances are fairly accurate. Also, now the initiation rates estimated from the model agree satisfactorily with the overall termination rate (sum of the alkenes). Our conclusion is that the model describes the data to a good first approximation, but falls short of perfection when the data are scrutinized in detail. Further work on this problem is indicated.

Recently Wang *et al.* (*9b*) carried out a related study of the effects of extralattice alumina formed by steaming on the activity, stability, and selectivity of Y zeolites in the cracking of *n*-heptane. Although a detailed product distribution was not given, their results were in substantial agreement with ours (particularly our *n*-pentane cracking data). The rates of cracking, of isomerization, of hydrogen transfer, and of coking all passed through maxima with lattice aluminum concentrations between 35 and 40 Al/u.c., whereas our maxima, like those of Lunsford and co-workers (*10*), fell between 30 and 35. Extra-framework alumina had a pronounced promoting effect on all the preparations except those containing <15 Al/u.c. We found a similar situation as that shown in Fig 1. Differences in the two studies should also be noted. Our samples were as nearly free of Na^+ as we could make them; theirs contained important amounts which are known to greatly reduce the catalytic activity (*4a, 7, 10c*). Also their reactant was *n*-heptane and ours were *n*-pentane and i-butane. Similarly, Wielers *et al.* (*15*) considered the cracking of *n*-hexane to be affected by zeolite structure, lattice aluminum concentration, and temperature. They reported that the relative contribution of the monomolecular protolytic cracking increased with increasing temperature (as did Haag and co-workers (*5*)), decreasing pore dimensions, and decreasing aluminum content. Our chain lengths should reflect the increasing importance of the bimolecular cracking of *n*-pentane, but no dependence on lattice aluminum concentration was observed over the Y zeolites investigated. Wielers *et al.* (*15*) used HZSM-5 catalysts covering a much broader range of composition. These data round out the literature and demonstrate the considerable consistency that has been evolved.

ACKNOWLEDGMENTS

Financial support from the U.S. Department of Energy, Division of Chemical Sciences, Office of Basic Energy Research under Grant DE-FG02-87ER13774A000 is gratefully acknowledged.

REFERENCES

1. (a) Abbot, J., and Wojciechowski, B. W., *J. Catal.* **115,** 1 (1989); (b) **113,** 353, (1988); (c) Wojciechowski, B. W., and Corma, A., "Catalytic Cracking; Catalysts, Chemistry and Kinetics," p. 147. Dekker, New York, 1986; (d) Abbot, J., and Wojciechowski, B. W., *J. Catal.* **104,** 80 (1987); (e) **107,** 451 (1987); (f) **109,** 274 (1988); (g) **115,** 521 (1989).
2. (a) Lombardo, E. A., Pierantozzi, R., and Hall, W. K., *J. Catal.* **110,** 171 (1988); (b) Lombardo, E. A., and Hall, W. K., *J. Catal.* **112,** 565 (1988); (c) Lombardo, E. A., Gaffney, T. R., and Hall, W. K., *in* "Proceedings, 9th International Congress on Catalysis, Calgary, 1988" (M. J. Phillips and M. Ternan, Eds.), Vol. 1, p. 114. Chem. Institute of Canada, Ottawa, 1988.
3. (a) Lombardo, E. A., Sill, G. A., and Hall, W. K., *J. Catal.* **119,** 426 (1989); (b) Hall, W. K., Lombardo, E. A., and Engelhardt, J., *J. Catal.* **115,** 611 (1989); (c) Lombardo, E. A., and Hall, W. K., *J. Catal.* **112,** 565 (1988).
4. (a) Engelhardt, J., and Hall, W. K., *J. Catal.* **125,** 472 (1990); (b) Shigeishi, R., Garforth, A., Harris, I., and Dwyer, *J. Catal.*, **130,** 423 (1991); (c) Bizreh, Y. W., and Gates, B. C., *J. Catal.* **88,** 240 (1984); Kannila, H., Haag, W. O., and Gates, B. C., *J. Catal.* **135,** 115 (1992).
5. (a) Haag, W. O., and Dessau, R. M., *in* "Proceedings, 8th International Congress on Catalysis, Berlin, 1984," Vol. 2, p. 305. Dechema, Frankfurt-am-Main, 1984; (b) Haag, W. O., *in* "Proceedings, 6th International Zeolite Symposium, Tokyo" (D. H. Olson and A. Bisio, Eds.), p. 466. Butterworths, London, 1984; (c) Haag, W. O., and Chen, N. Y., *in* "Catalyst Design—Progress and Perspectives" (L. L. Hegedus, Ed.), p. 163. Wiley, New York, 1987.
6. (a) Garralon, G., Corma, A., and Fornes, V., *Zeolites* **9,** 84 (1989); **7,** 559 (1987); (b) Corma, A., Fornes, V., and Ortega, E., *J. Catal.* **92,** 284 (1985); (c) Corma, A., *in* "Zeolites: Facts, Figures, Future" (P. A. Jacobs and R. A. van Santen, Eds.), Part A, p. 49ff. Elsevier, Amsterdam/New York, 1989.
7. (a) McVicker, G. B., Kramer, G. M., and Ziemiak, J. J., *J. Catal.* **83,** 286 (1983); (b) Bayerlein, R. A., McVicker, G. B., Yacullo, L. N., and Ziemiak, J. J., *J. Phys. Chem.* **92,** 1967 (1988).
8. Brenner, A., and Emmett, P. H., *J. Catal.* **75,** 410 (1982).
9. (a) Shertukde, P. V., Hall, W. K., Dereppe, J. M., and Marcelin, G., Submitted for publication; (b) Wang, Q. L., Giannetto, G., Torrealba, M., Perot, G., Kappenstein, C., and Guisnet, M., *J. Catal.* **130,** 459, 471 (1991).
10. (a) Sohn, J. R., DeCanio, S. J., Fritz, P. O., and Lunsford, J. H., *J. Phys. Chem.* **90,** 4847 (1986); (b) DeCanio, S. J., Sohn, J. R., Fritz, P. O., and

Lunsford, J. H., *J. Catal.* **101,** 132 (1986); (c) Fritz, P. O., and Lunsford, J. H., *J. Catal.* **118,** 85 (1989); (d) Lunsford, J. H., *ACS Symp. Ser.* **35**(4), 654 (1990).

11. Lago, R. M., Haag, W. O., Mikowski, R. J., Olson, D. H., Bellring, S. D., Schmitt, K. D., and Kerr, G. T., *in* "New Developments in Zeolite Science and Technology" (Y. Murakami *et al.*, Eds.), Studies in Surface Science and Catalysis, Vol. 28, p. 677. Elsevier, Amsterdam, 1986.

12. Hall, W. K., Engelhardt, J., and Sill, G. A., *in* "Zeolites: Facts, Figures, Future" (P. A. Jacobs and R. A. van Santen, Eds.), Elsevier, p. 1253ff. Amsterdam, 1989.

13. Brunner, E., Ernst, H., Freude, D., Froehlich, T., Hunger, M., and Pfeifer, H., *J. Catal.* **127,** 54 (1991).

14. (a) Olah, G. A., Surya Prakash, G. K., and Sommer, J., *in* "Superacids" Wiley, New York, 1985; (b) Olah, G. A., Halpern, Y., Shen, J., and Mo, Y. K., *J. Am. Chem. Soc.* **93,** 1251 (1971); (c) *J. Am. Chem. Soc.* **95,** 4960 (1973); (d) Plannelles, J., Sanchez-Marin, J., Tomas, F., and Corma, A., *J. Mol. Catal.* **32,** 365 (1985).

15. Wielers, A. F. H., Vaarkamp, M., and Post, M. F. M., *J. Catal.* **127,** 51 (1991).

16. Umanski, B., Engelhardt, J., and Hall, W. K., *J. Catal.* **127,** 128 (1991).